Journal of Materials, Processes and Environment
May edition. Vol. 5. N° 1. (2017)
ISSN : 2335-1020

Adsorption of Malachite Green (MG) onto Apricot Stone Activated Carbon (ASAC)-Equilibrium, kinetic and thermodynamic studies

Moussa ABBAS [1], Tounsia AKSIL[2]

(1) Laboratory of Soft Technologies and Biodiversity (LTDVPMBB), Faculty of Sciences, University M'hamed Bougara of Boumerdes, 35000 Algeria.

(2) University M'hamed Bougara of Boumerdes, Faculty of Sciences, Chemical Department 35000 Algeria.

Abstract —The adsorption of malachite green (MG) onto apricot stone activated carbon (ASAC) in a batch adsorber and the effects of contact time, initial pH, agitation speed, adsorbent dosage and initial dye concentration on the MG adsorption by the ASAC have been studied. It was observed that under optimized conditions up to 23.94 mg/g at 25 °C and 88.5 mg/g at 70 °C could be removed from solution. Kinetic parameters; rate constants, equilibrium adsorptin capacities and correlation coefficients, for each kinetic equation were calculated and discussed. It was shown that the adsorption of MG onto ASAC could be described by the pseudo second-order equation. The experimental isotherm data were analyzed using the Langmuir, Freundlich, Temkin, Elovich and Redlich-Peterson equations. Adsorption of MG onto ASAC followed the Langmuir isotherm. The evaluation of thermodynamics parameters such as the negative Gibbs free energy and positive enthalpy change indicated respectively the spontaneous and endothermic nature of the reaction and the chimisorption of the sorption process.

Keywords: Kinetic, Isotherm, Adsorption, Thermodynamic, Apricot stone, Malachite green

1. Introduction

The effluents from the textile, leather, food processing, dyeing, cosmetics, paper and dye manufacturing industries are important sources of pollution **[1].** Many dyes and their break down products may be toxic for living organisms particularly malachite green (MG) **[2].** Therefore, decolorizations of dyes are important aspects of wastewater treatment before their discharge in the aquatic environment. It is difficult to remove the dyes from such effluents, because they are not easily degradable and are generally not removed from wastewater by the conventional techniques **[3].** Presence of dyes in water gives rise to a chemical oxygen demand, biochemical oxygen demand and high-suspended solids. Colored wastewaters arise as a direct result of the production of dyes and also as a consequence of their use in the textile and others industries. Considering volume discharged and effluent combustion, the wastewaters from the textile industry are rated as the most polluting among all industrial sectors. Their presence in water, even at very low concentrations, is highly visible and undesirable and may dramatically affect the photosynthetic activity in the aquatic life due to reduced light penetration. In our day, various physical-chemical techniques have been studied to assess their applicabilities for the treatment of this type of industrial discharge. Among these processes may be included coagulation, adsorption, precipitation, flocculation and ozonation. The adsorption is considered to be an effective method for the removal of dyes due to its low maintenance, simple operation and removal effectiveness. Moreover, it provides an attractive alternative, especially if the adsorbent is inexpensive and readily available.

Activated carbon is the versatile adsorbent and has been used regularly for the adsorption process, but remains expensive. Consequently, many investigators have studied the feasibility of various low cost and abundantly available substances that are used for the synthesis of activated carbon. Therefore, in recent years, this has prompted a growing research interest in the production of activated carbons from renewable and cheaper precursors which are mainly industrial and agricultural by-products, for the wastewater treatment. However, the available activated carbons in commerce are relatively expensive, their production and regeneration cost may constitute limiting factors**.** Hence, most researchers worldwide have focused on the search of new low-cost precursors especially issued from agricultural wastes such as rubber seed coat **[4]**, pecan shells **[5]**, olive stones **[6]**, pine wood **[7]**,

Corresponding author : Moussa ABBAS
Adress LTDVPMBB, University o Boumerdès
E-mail: moussaiap@gmail.com

sawdust **[8]**, coir pith **[9]**, rice husk **[10]**, bamboo **[11]** and apricot stone **[12]**. The remarkable adsorption capacity of activated carbons is due to their well-developed porous structure and pore size distribution, as well as the surface functional groups. Agricultural by-products exist in large amounts and about 20.000 tonnes of apricot stones per year are produced in Algeria **[13] (Table 1)**. Over the past, these by-products were used as fuel in rural areas but now the preparation of activated carbon is considerably encouraged. Apricot stone is a cheap precursor for activated carbon source. Therefore, it is important to evaluate its performance as adsorbent **[14]**. The advantage of the utilization of an abundant and available residual biomass namely the apricot stone, as a raw material for activated carbons gives an additional economical interest to the technical studies. The apricot stone used in the present study was prepared by chemical and physical activation and this study was carried out with the aim to optimize conditions such as initial dye concentration, pH, particle size, contact time, adsorbent dosage, agitation speed and temperature.

2. Experimental

2.1. Materials and methods

Analytical grade reagents are used in all experiments. Basic dye, MG (99 %) is purchased from Merck Company. Aactivated carbon was prepared by a conventional method: carbonization and chemical activation with phosphoric acid as follows: Apricot stones obtained from Boumerdes region are air-dried, crushed and screened to obtain two fractions with geometrical mean sizes of 63 and 2.5 mm. 100 g of the selected fraction are impregnated with concentrated H_3PO_4 (85%) and dried in air. Then, it is activated in a muffle furnace oven at 250 °C (4h). The clean biomass is mechanically ground and sifted to get powders of different particle sizes: < 63 µm to 2 mm.

Activated carbon characterization

The prepared activated carbon was characterized by selected physical properties (bulk density and surface area), chemical and adsorption properties (point of zero charge: pH_{pzc}). The elemental analysis was performed by using an elemental analyzer LECO-CHNS 932. The specific surface area of the activated carbon was achieved by using the BET-technique, as a sorption phenomenon of nitrogen gas on the adsorbent surface, at 77 K. The measurements were made using a Pore Size Micrometric-9320, USA equipment. The ash content Ash (%) of the activated carbon was determined by using a muffle furnace over 3 h at 450 °C. The conductivity measurements were carried out with a conductimeter type Erwika.The pH_{pzc} of the ASAC was determined by using potassium nitrate. 20 mL of a KNO_3 solution (0.01 M) were placed in different closed conical flasks. The pH of each solution in flask has been adjusted between 2 and 14 by adding solutions of HCl (0.1 M) or NaOH (0.1 M). Then, 0.1 g of ASAC was added and the final pH was measured after 24 h under agitation at room temperature. The pH_{pzc} is the point where the curve of final pH versus initial pH crosses the line: final pH = initial pH.

The infrared analysis of the prepared ASAC was performed by using an IR spectrophometer of FT Bomen-Michelson type. The IR spectrum was obtained by grinding 2 mg of the ASAC sample with 98 mg of spectroscopic KBr. The mixture was pressed at elevated pressure into a small disc of 1 cm in diameter and 2 mm in thickness.

Batch mode adsorption studies

The effects of the experimental parameters such as the initial MG concentration (4-20 $mg.L^{-1}$), pH (1-14), adsorbent dosage (1-10 g L^{-1}), agitation speed (100-1200 rpm) and temperature (298-323 K) on the adsorptive removal of MG ions are studied in a batch mode of operation for a variable specific period of contact time (0-60 min). The MG solutions are prepared by dissolving the accurate amount of MG (99 %) in distilled water, used as a stock solution and diluted to the required initial concentration; pH is adjusted with HCl (0.1 mol L^{-1}) or NaOH (0.1 mol L^{-1}). For the kinetic studies, desired quantities of ASAC is contacted with 10 mL of MG solutions in Erlenmeyer flasks. Then, the flasks are placed on a rotary shaker at 300 rpm and the samples are taken at regular time intervals and centrifuged at 3000 rpm for 10 min. The MG content in the supernatant was analyzed on a Perkin Elmer UV-visible spectrophotometer model 550S at (λ_{max} = 494 nm). The amount of MG ions adsorbed by activated carbon q_t ($mg.g^{-1}$) is calculated by using the following equation (A1):

$$q_t = \frac{(C_0 - C_e)\cdot V}{m} \qquad \textbf{(A1)}$$

Where C_o is the initial MG concentration and C_t the MG concentrations ($mg.L^{-1}$) at any time, V the

volume of solution (L) and m the mass of the activated carbon (g). Due to the inherent bias resulting from linearization of the isotherm models, the non-linear regression Root Mean Square Error (RMSE) equation (A2), the Sun of Error Squares (SSE) equation (A3) and Chi-Squares (X^2) equation (A4) test are employed as criterion for the quality of fitting **[6]**.

$$\mathbf{RMSE} = \sqrt{\frac{1}{N-2} \cdot \sum_1^N (q_{e,exp} - q_{e,cal})^2} \qquad \textbf{(A2)}$$

Where, $q_{e(exp)}$ ($mg.g^{-1}$) is the experimental value of uptake, $q_{e(cal)}$ the calculated value of uptake using a model ($mg.g^{-1}$) and N the number of observations in the experiment (the number of data points). The smaller RMSE value indicates the better curve fitting **[14]**.

3. Results and Discussion

Characterization of the prepared ASAC

The physical and chemical properties of ASAC and the elementary analysis are summarized in **Table 1**.

Structural characterization by infrared spectroscopy

The spectra of the adsorbent display a number of absorption peaks, indicating that many functional groups are present in the adsorbent **[23]**. Peaks are observed at 3436, 2929, 1732, 1599 and 1508 cm^{-1}.

Table. 1: Physical and chemical properties of the apricot stones activated carbon (ASAC).

Elemental analysis (%)	C : 48.45	H : 6.03	N : 0.44	O : 45.08

pH_{zpc}	7.06
Surface area (m^2/g)	88.05
Average pore diameter (Å)	176.3
Average pore volume (mL/g)	0.264
Conductivity (µS/cm)	112

Humidity (%)	1.48
The rate of ash (%)	1.68
The percentage of organic matter (%)	98.32

3.1. Effect of analytical parameters

. In the first stage of batch adsorption experiments on ASAC, the effect of particle sizes on the acid dye adsorption by ASAC is examined. Significant variations in the uptake capacity and removal efficiency were observed at different particles sizes, indicating that the best performance is obtained with lower particle sizes (315-800 µm). In general, smaller particles provide large surface area, resulting in high acid dye uptake capacity and removal efficiency. The particle size range (315-800 µm) is subsequently used in all adsorption experiments. The pH of the MG solution plays an important role in the adsorption process**.** It is evident that the percentage of acid dye removal increases consistently with decreasing pH. The effect of pH on the adsorption by ASAC can be explained on the basis of the point of zero charge pH_{zpc}, for which the adsorbent surface is neutral. The surface charge of the adsorbent is positive when the medium pH is under pH_{zpc} and negative for higher pH pH_{zpc} of ASAC is 7.05 and the surface charge of ASAC is negative at higher pH. As the pH decreases, the number of positively charged sites increases and favours the adsorption of MG ions by electrostatic. The maximum uptake was obtained for a speed of 300 rpm. Such moderate speed gives a good homogeneity for the mixture suspension.

The adsorption capacity of MG increases with time and attains a maximum after 40 min and thereafter and reaches a constant value, indicating that no more MG ions are further removed from the solution. The equilibrium time is found to be 40 min. The initial concentration of acid dye from 50 to 100 $mg.L^{-1}$, leads to increased adsorbed amount from 10.08 to 34.51 $mg.g^{-1}$. For the first stage of batch adsorption experiments on (ASAC),

the effect of adsorbent dosage on the acid dye adsorption is examined. Significant variations in the uptake capacity and removal efficiency observed at different adsorbent dosages (1-10 $g.L^{-1}$) indicate that the best performance is obtained with a dosage of 1 $g.L^{-1}$.

3.2 Adsorption Isotherms

The shape of the isotherms is the first experimental tool to diagnose the nature of a specific adsorption phenomenon. The isotherms have been classified according to Giles et al. **[15]** in four main groups: L, S, H, and C, and the isotherm of ASAC at different temperatures (25 ^{o}C and 65 ^{o}C) displays both L type curves **(Fig. 1).** The initial part of the L curve indicates a small interaction between the basic dye and the carrier at low concentrations. However, as the concentration in the liquid phase increases, the adsorption occurs more readily. This behaviour is due to a synergistic effect, with the adsorbed molecules facilitating the adsorption of additional molecules as a result of attractive interaction adsorbate-adsorbate. Equilibrium isotherm equations are used to describe the experimental adsorption data. The equation parameters and the underlying thermodynamic assumptions of these equilibrium models often provide some insights into both the sorption mechanism and the surface properties and affinity of the adsorbent.

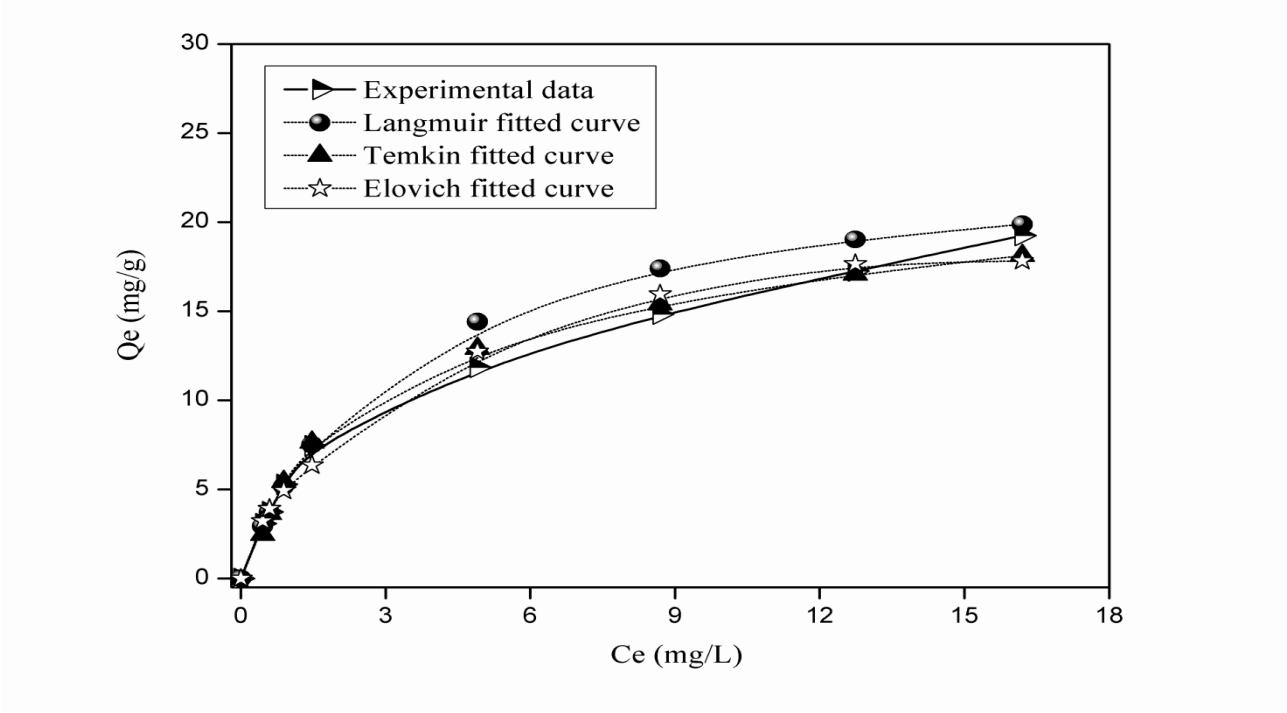

Figure. 1: Adsorption isotherm of MG by ASAC at temperature 25 °C.

The initial part of the L curve indicates a small interaction between the basic dye and the carrier at low concentrations. However, as the concentration in the liquid phase increases, the adsorption occurs more readily. This behaviour is due to a synergistic effect, with the adsorbed molecules facilitating the adsorption of additional molecules as a result of attractive interaction adsorbate-adsorbate. Equilibrium isotherm equations are used to describe the experimental adsorption data. The equation parameters and the underlying thermodynamic assumptions of these equilibrium models often provide some insights into both the sorption mechanism and the surface properties and affinity of the adsorbent. The importance of obtaining the best fit isotherm becomes more and significant, because as more applications are developed, more accurate and detailed isotherm descriptions are required for the adsorption system designs.

The Langmuir equation **[16]** is the best known and most widely applied, it is represented by the linear form:

$$\frac{1}{q_e} = \frac{1}{q_{max}} - \frac{1}{q_{max} . K_L . Ce} \qquad \textbf{(B1)}$$

Where C_e is the equilibrium concentration ($mg.L^{-1}$), q_{max} the monolayer adsorption capacity (mg/g)

and K_L the constant related to the free adsorption energy (Langmuir constant, $L.mg^{-1}$). The applicability to the adsorption study is compared by evaluating the statistic RMSE values. The smaller RMSE values obtained at 25 °C for the models indicate a better fitting. The essential features of the Langmuir isotherm **Figs.2a and 2b** can be expressed in terms of dimensionless constant called separation factor, defined by the following equation (B2) **[17].**

$$R_L = \frac{1}{1+K_L \cdot C_0} \qquad \textbf{(B2)}$$

Where C_o the initial concentration of the adsorbate in solution. The R_L indicates the type of isotherm: irreversible (R_L = 0), favourable (0 < R_L < 1), linear (R_L = 1) or unfavourable (R_L > 1). In this study, the R_L values are less than 1, thus confirming that the adsorption process is favoured in both cases as well as the applicability of Langmuir isotherm.

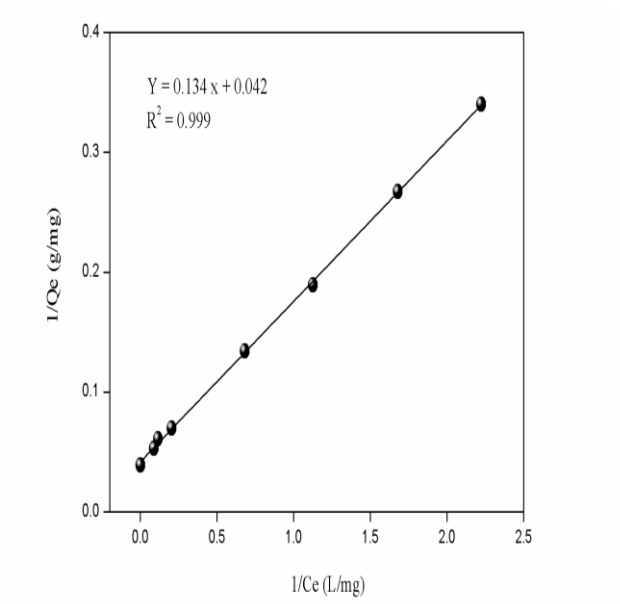

Figure .2a: The Langmuir isotherms (I) for the adsorption of MG ions onto ASAC.

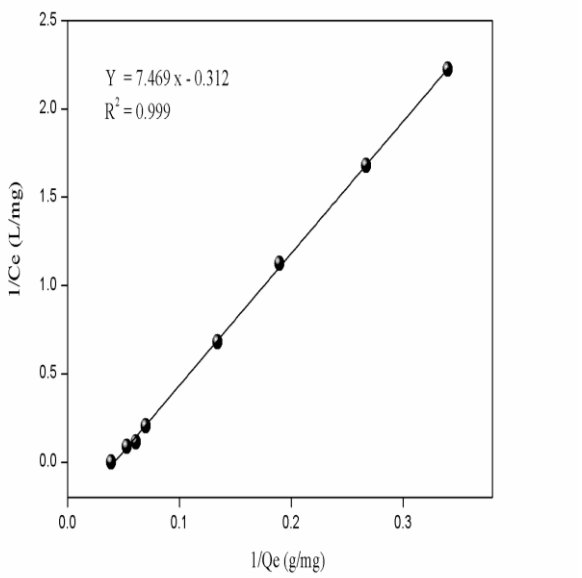

Figure .2b: The Langmuir isotherms (V) for the adsorption of MG ions onto ASAC

The Freundlich isotherm can be applied to nonideal adsorption on heterogeneous surfaces as well as multilayer sorption; is expressed by the following equations (B3) **[16].**

$$\mathbf{Ln\, q_e = Ln\, K_F + \frac{1}{n} \cdot Ln\, Ce} \qquad \textbf{(B3)}$$

The constant K_F indicates the adsorption capacity of the adsorbent ($L.g^{-1}$) and n is an empirical constant related to the magnitude of the adsorption driving force. Therefore a plot of Lnq_e versus LnC_e enables the determination of the constant K_F and exponent n.

The Temkin isotherm describes the behavior of adsorption systems on heterogeneous surfaces, and it has generally been applied in the following form equation (B4) **[18].**

$$\mathbf{Qe = \frac{RT}{b} LnA + \frac{RT}{b} LnCe = BLnA + BLn\, Ce} \qquad \textbf{(B4)}$$

The adsorption data can be analyzed according to equation (B4). Therefore, a plot of qe versus LnCe enables to determine the constants A and B. The Elovich isotherm **[19]** is based on the principle of the kinetic assumes that the number of adsorption sites increases exponentially with the adsorption, which implies a multilayer adsorption described by equation (4).

$$\mathbf{Ln\, \frac{q_e}{C_e} = Ln\, q_m \,.K_E\, \frac{q_e}{q_m}} \qquad \textbf{(B5)}$$

Where K_E ($L.mg^{-1}$) is the Elovich and Harkins constant at equilibrium, q_m ($mg.g^{-1}$) the maximum adsorption capacity, q_e ($mg.g^{-1}$) the adsorption capacity at equilibrium and C_e ($g.L^{-1}$) the concentration of the adsorbate at equilibrium. If the adsorption is described by the equation of Elovich, the equilibrium constant and the

maximum capacity can be calculated from the plot of Ln (q_e/C_e) versus q_e.

The theoretical parameters of adsorption isotherms along with the regression coefficients, RMSE, SSE and X^2 are listed in **Table 2**. The Langmuir isotherm model exhibits the higher RMSE, X^2 and SSE values.

Table .2: Sorption isotherms coefficients of different models.

Temperature		T = 25 °C	T = 70 °C
Model		Parameters	
Langmuir (I)	1/Qe = f (1/Ce)	Q_{max} : 23.80 mg/g K_L : 0.313 L/mg R^2 : 0.999 X^2 : 0.188 SSE : 0.35 RMSE : 0.59	Q_{max} : 83.33mg/g K_L : 0.0085 g/mg R^2 : 0.999 X^2 : 0.208 SSE : 0.39 RMSE : 0.72
Langmuir (V)	1/Ce = f (1/Qe)	Q_{max} : 23.94 mg/g K_L : 0.312 L/mg R^2 : 0.999 X^2 : 0.185 SSE : 0.37 RMSE : 0.61	Q_{max} : 88.5 mg/g K_L : 0.0088 g/mg R^2 : 0.999 X^2 : 0.207 SSE : 0.38 RMSE : 0.68
Freundlich	LnQe = f(LnCe)	K_F : 2.199 mg/g 1/n : 1.917 R^2 : 0.989 X^2 : 212.33 SSE : 14787.9 RMSE : 121.61	K_F : 0.922 mg/g 1/n : 0.845 R^2 : 0.996 X^2 : 256.33 SSE : 15678.9 RMSE : 128.61
Elovich	Ln(Qe/Ce) = f (qe)	Q_{max} : 8.62 mg/g K_L : 1.198 g/mg R^2 : 0.984 X^2 : 0.064 SSE : 0.092 RMSE : 0.303	Q_{max} : 142.8 mg/g K_L : 0.0088 g/mg R^2 : 0.89 X^2 : 0.123 SSE : 10.125 RMSE : 1.36
Temkin	Qe = f (LnCe)	K_T : 3.904 L/mg β_T : 4.37 ΔQ : 13.556 kj/mol β_T : $RTQ_m/\Delta Q$ R^2 : 0.987 X^2 : 0.055 SSE : 0.036 RMSE : 0.189	K_E : 0.2028 L/mg β_T : 10.028 ΔQ : 25.167 kj/mol β_T : $RTQ_m/\Delta Q$ R^2 : 0.948 X^2 : 0.066 SSE : 0.055 RMSE : 2.189
Redlich-Peterson	Ce/Qe = f (C_e^n)	K : - 3.904 g/L Qm : 8.88 mg/g R^2 : 0.993 X^2 : 1.236 SSE : 10.236 RMSE : 7.125	

3.3. Adsorption kinetics

The kinetic study is important for the adsorption process, it describes the uptake rate of adsorbate and controls the residual time of the whole adsorption process. Two kinetic models namely the pseudo first order and pseudo second-order are selected in this study to describe the adsorption.

- The pseudo first order equation **[20]** is given in equation (C1):

$$\log(q_e - q_t) = \log q_e - \frac{K_1}{2.303} \cdot t \qquad \textbf{(C1)}$$

- The pseudo second order model **[21]** is expressed by the equation (C2):

$$\frac{t}{q_t} = \frac{1}{K_2 \cdot q_e^2} + \frac{1}{q_e} \cdot t \qquad \textbf{(C2)}$$

Where q_t (mg.g^{-1}) is the amount of metal adsorbed on the adsorbent at various times t (min), K_1 the rate constant of the pseudo-first order kinetic (min^{-1}), K_2 the rate constant of the pseudo-second order kinetic (g.mg^{-1} min^{-1}). For the pseudo-first order kinetic, the experimental data deviate greatly from linearity. This was evidenced by the low values of q_e and determination coefficients. Therefore, the pseudo-first order model is inapplicable to this system. The determination coefficient and $q_{e,cal}$ of the pseudo-second order kinetic model are in good agreement with the experimental results **(Table 3)**.

Table. 3: Kinetic parameters for adsorption of MG ions onto ASAC

	2^{ieme}	Ordre				1^{ier}	Ordre		
C_o (mg/L)	Q_{ex} (mg/g)	Q_{cal} (mg/g)	R^2	ΔQ/Q (%)	K_2 (g/mg.mn)	Q_{cal} (mg/g)	R^2	ΔQ/Q (%)	K_1 (mn^{-1})
4.45	3.31	3.460	0.999	4.33	0.1218	1.96	0.923	40.78	0.045
13.5	6.44	6.757	0.999	4.69	0.0633	3.97	0.959	38.35	0.054
17.6	8.23	8.40	0.999	2.02	0.1042	3.53	0.889	55.95	0.053

		Elovich			Diffusion			
C_o (mg/L)	R^2	β (g/mg)	α (mg/g.mn)	C_o (mg/L)	K_{in} mg/gmn$^{1/2}$	R^2	C (mg/g)	D Cm^2/s
4.45	0.795	1.4802	2.418	2	0.682	0.928	0.5828	
13.5	0.885	0.9525	12.493	5	1.337	0.979	1.0742	0.5210^{-7}
17.6	0.787	1.1169	234.69	10	1.267	0.808	3.4100	

3.4. Intraparticle diffusion study

An empirically found functional relationship common to most adsorption process is that varies almost proportionally with $t^{1/2}$, the Weber-Morris plot (q_t versus $t^{1/2}$), rather than with the constant time t **[22]** equation **(D1).**

$$q_t = K_{in}\, t^{1/2} + C \qquad \textbf{(D1)}$$

Where K_{in} is the intraparticle diffusion rate constant. Values of intercept C gives an idea about the thickness of boundary layer**.** The values of K_{in} and C obtained from the slope and intercept of linear plots and the constant of the Elovich model are listed in **Table.4.** The adsorption

mechanisms and the kinetics can be described according to several models, which can predict the breakthrough curves at different times and accuracies. However, there are not clear criteria to estimate which is the most convenient for a given case, and a lot of concerns must be considered: The mass transfer resistances involved relation type between the adsorbed amount and the diffusion coefficients. It is well known that a well carried out batch experiment should give valuable data to estimate the diffusion coefficients. Usually, in the real conditions, the mass transport resistance inside the solid is very much higher than through the external fluid film on the solid particles.

Table. 4: Kinetic parameters for adsorption of MG ions onto ASAC

	2^{ieme}	Ordre				1^{ier}	Ordre		
C_o (mg/L)	Q_{ex} (mg/g)	Q_{cal} (mg/g)	R^2	ΔQ/Q (%)	K_2 (g/mg.mn)	Q_{cal} (mg/g)	R^2	ΔQ/Q (%)	K_1 (mn^{-1})
4.45	3.31	3.460	0.999	4.33	0.1218	1.96	0.923	40.78	0.045
13.5	6.44	6.757	0.999	4.69	0.0633	3.97	0.959	38.35	0.054
17.6	8.23	8.40	0.999	2.02	0.1042	3.53	0.889	55.95	0.053

		Elovich			Diffusion			
C_o (mg/L)	R^2	β (g/mg)	α (mg/g.mn)	C_o (mg/L)	K_{in} $mg/gmn^{1/2}$	R^2	C (mg/g)	D Cm^2/s
4.45	0.795	1.4802	2.418	2	0.682	0.928	0.5828	
13.5	0.885	0.9525	12.493	5	1.337	0.979	1.0742	0.5210^{-7}
17.6	0.787	1.1169	234.69	10	1.267	0.808	3.4100	

3.5. Effect of temperature

The thermodynamic parameters i.e. the free energy (ΔG^o), enthalpy (ΔH^o) and entropy (ΔS) are determined from the following equations **(E1)** and **(E2) [23, 24]**.

$$\mathbf{\Delta G^o = - RT\ LnK} \qquad \mathbf{(E1)}$$

$$\mathbf{\Delta G^o = \Delta H^o - T\Delta S^o} \qquad \mathbf{(E2)}$$

The thermodynamic equilibrium constant K for the sorption was determined by M. Ghaedj et al.**[25]** by plotting q_e/C_e versus C_e and extrapolating to zero q_e. The ΔH^o and ΔS^o values obtained from the slope and intercept of Van't Hoff plots of LnK versus 1/T and the ΔG^o values at various temperatures are summarized in **Table 5.**

Table. 5 : Thermodynamic parameters for the MG adsorption on ASAC

T (K)	1/T (K^{-1})	K	Ln K	ΔG^o (KJ/mol)	ΔH^o (KJ/mol)	ΔS^o (J/mol.K)
298	0.00336	1.04	0.047	- 0.191		
306	0.00327	1.76	0.569	- 1.539		
313	0.00319	2.83	1.04	- 2.737	50.86	171.09
323	0.00309	5.32	1.67	- 4.447		

3.6. Performance of the prepared ASAC

In order to have an idea about the efficiency of the prepared ASAC, a comparison of basic dye adsorption of this work and other relevant studies is reported in **Table 6**. The adsorption capacity (q_{max}) is the parameter used for the comparison. One can conclude that the value of q_{max} is in good agreement with those of most previous works, suggesting that MG could be easily adsorbed on ASAC prepared in this work. This indicates that the apricot stone, very abundant in Algeria, is a cheap and effective adsorbent for the MG. ASAC is promising adsorbent for metals and basic dyes owing to pHpzc and our perspective is achieve the adsorption tests in column mode using industrial effluents. Such results are currently under way and will be reported in a next future.

Table. 6: Comparison of ASAC performances with precursors from previous studies.

Adsorbent	Q_{max} (mg/g)	References
Activated Carbon	500	**[26]**
Bagasse Fly Ash	170.3	**[27]**
Jute Fiber Carbon	136.6	**[28]**
Biomass of Phitophora	117.6	**[29]**
Activated Carbon (Waste Apricot)	116.3	**[30]**
Cyclodextrin-Based Adsorbent	91.9	**[31]**
Activatd Slag	76.2	**[32]**
Hen Feathers	10.7	**[33]**
Iron Humate	19.2	**[34]**
Arundo Domax Root Carbon	8.69	**[35]**
Bentonite Cly	7.72	**[36]**
Sugar Cane Dust	4.88	**[37]**
Activated Charcoal	0.18	**[38]**
Lemon Peel	51.73	**[39]**
Zeolite	46.35	**[40]**
Caulerpa Racemosavar Cylindracea CRC	25.67	**[41]**
Bamboo-based Activated Carbon	263.6	**[42]**
Groundnut Shell based Activated Carbon	222.2	**[43]**
Commercial Activated Carbon	8.27	**[44]**
Laboratory Grade Activated Carbon	42.18	**[44]**
Bentonite	178.6	**[49]**
Rubber Wood Sawdust	36.3	**[46]**
Functionalized Sawdust	126.1	**[47]**
Dead Tree Leaves	89.4	**[48]**
Apricot Stone activated carbon (ASAC)	23.94 at 25 ^{o}C	**This Study**
…… (ASAC)	88.50 at 70 ^{o}C	**.**

4. Conclusions

. This study has shown that the activated carbon prepared from apricot stone can be employed as effective adsorbent for the removal of MG from aqueous solution.

. The Langmuir isotherms model provided a better fit of the equilibrium adsorption data one. They gave a maximum adsorption capacity of 34.51 $mg.g^{-1}$ at 25 ^{o}C which decreased down to 23.08 $mg.g^{-1}$ at 70 ^{o}C at pH 13. The pseudo-second order model proved the best description of the kinetic data.

. The negative value of ΔG^{o} and positive value of ΔH^{o} indicate that the adsorption of MG onto ASAC is spontaneous and endothermic over the studied range of temperatures.

. The positive value of ΔS^{o} states clearly that the randomness increases at the solid-solution interface during the MG adsorption onto ASAC, indicating that some structural exchange may occur among the active sites of the adsorbent and the ions.

. The adsorption of MG ions by ASAC follows a pseudo-second order kinetic model, which relies on the assumption that chemisorptions may be the rate-limiting step. In chemisorption, the MG ions are attached to the adsorbent surface by forming a chemical bond and tend to find sites that maximize their coordination number with the surface.

. The kinetics and thermodynamic data can be further explored for the design of an adsorber for industrial effluents treatment.

. Acetic acid has been found effective for the regeneration of adsorbent than other solvents. It was noted during the experiments in the laboratory in batch mode that the adsorbent regenerated after

several washings showed a decrease of the adsorption capacity (40 %) can be used again efficiently for subsequent use.

. This study in tiny batch gave rise to encouraging results, and we wish to achieve the adsorption tests in column mode under the conditions applicable to the treatment of industrial effluents

and the present investigation showed that ASAC is a potentially useful adsorbent for the metals, acid and basic dyes.

References

[1] M. Abbas et al; Desalination and water treatment **(2015)** 1-12

[2] N. Kannan and M.M Sundaram., Dyes and Pigments 51**(2001)** 25-40.

[3] M. Isık and D.T Sponza, , Process Biochemistry, 40 **(2005)** 1053-1062.

[4] S. Rengaraj, S.H. Moona, R. Sivabalan, B. Arabindoo, V. Murugesan, J. Hazard. Mater.B89 **(2002)** 185–196.

[5] R.A. Shawabkeh, D.A. Rockstraw, R.K. Bhada, Carbon 40 **(2002)** 781–786.

[6] A.H. El-Sheikh, A.P. Newman, H.K. Al-Daffaee, S. Phull, N. Cress, J. Anal. Appl. Pyrolysis 71 **(2004)** 151–164.

[7] R.L. Tsenga, F.C. Wub, R.S. Juang, Carbon 41 **(2003)** 487–495.

[8] P.K. Malik, J. Hazard. Mater. B113 **(2004)** 81–88.

[9] C. Namasivayam, D. Kavitha, Dyes Pigments 54 **(2002)** 47–58.

[10] Y. Guo, J. Zhao, H. Zhang, S. Yang, J. Qi, Z. Wang, H. Xu, Dyes Pigments 66 **(2005)** 123–128.

[11] B.H. Hameed, A.T.M. Din, A.L. Ahmad, J. Hazard. Mater. 141 **(2007)** 819–825.

[12] L. Mouni et al, Desalination 276 **(2011)** 148-153

[13] FAO Annuaire de la production (2009). Ed FAO Rome

[14] M. Abbas et al; J. Ind. and Eng. Chem V 20 **(2014)** 745-751

[15] C. H. Giles, T. H. Mac Ewan, S. N. Nakhwa, D. Smith, J. Chem. Soc. 10 **(1960)** 3973-3993.

[16] C. Gerent, V.K.C. Lee, P. Le clorrek, G. McKay, Crit. Rev Environ. Sci. Technolol. V37 **(2007)** 41-121

[17] C. Crini, H.N. Peindy, F. Gimbert, Separ , Purif Technol. V53 **(2007)** 97-110

[18] S.J. Allen, G. McKay,J.F. Porter, J. Colloid Interface Sci. V280 **(2004)** 222-333

[19] A. Ozcan, E.M. Oncu, A.S. Ozcan, Colloids Surfaces A, Physico-Chem. Eng, Aspects V 277 **(2006)** 90-97

[20] S. Lagergren. K. Sven.Ventensskapsakad. Handlingar Band, V 24**(1998)**1-39.

[21] Y.S Ho, G. Mc Kay Water Res. V 34, (3) **(2000)** 735-742.

[22] M.J weber and J Morris ASCE journal Saint Engineering Division V 89(1963) 31-51.

[23] M. Abbas, S. Kaddour, M. Trari, . Journal of Industrial and Engineering Chemistry V20 (2014) 745–751.

[24] T-Y kin, S.-S. Park, S.Y. Cho. J. Ind. Eng. Chem. 18, 3 **(2012)** 1751

[25] M. Ghaedj, F. Karimi, B. Barrazzch, R. Saraei, A. Danichfar, J. Ind. Eng. Chem. V19, 3 **(2013)** 756

[26] K.V. Kumar,. Journal of Hazardous Materials B136 **(2006)** 197-202

[27] I.D. mall, V.C. Srivastava, G.V.A Kumar, I.M. Mishra, Colloids Surfaces A physic-chemistry Engineering Aspects V278 **(2006)** 175-187

[28] K. Porkodi, K.V. Kumar, Journal Hazardous Materials V143 **(2007)** 311-327

[29] K.V. Kumar, S. Sivanesan, V. Ramamurthy, Process Biochemistry V40 **(2005)** 2865-2875

[30] C.A. Basa,. Journal of Hazardous Materials B135 **(2006)** 232-241

[31] G. Crini, H. N Peindy, F. Gimbert and C. Robert. Separation and purification technology V53 **(2007)** 97-110

[32] K.V. Gupta, S.K Srivastava, D. mohan, , Industrial Engineering Chemistry Research 36 **(1997)** 2207-2218

[33] A. Mittal, Journal of Hazardous Materials B133 **(2006)** 196-233.

[34] P. Janos, Sorption of basic dyes onto iron humate. Environmental Science Technology V37 **(2003)** 5792-5798

[35] J. Zhang, LI. Yan, C. Zhang and Y. Jing,. Journal of Hazardous Materials V150 **(2008)** 774-782

[36] S.S Tahir, N.Rauf, Chemosphere V63 **(2006)** 1842-1848

[37] S.D Khattri, M.K Singh,. Adsorption Science Technology 17 **(1999)** 269-282

[38] M.J. Iqbal, M.N Ashiq, Journal of Hazardous Materials V139 **(2007)** 57-66

[29] K.V. Kumar, Optimum, Dyes Pigments V74 **(2007)** 595-597

[40] S.wang, E. Aiyanto, Journal colloid interface Science V314 **(2007)** 25-31

[41] Z. Bekci, Y.Seki, L. Cavas, , Journal of Hazardous Materials V161 **(2009)** 1454-1460.

[42] B.H. Hameed and M.I El Khaiary, Journal of Hazardous Materials V157 **(2008)** 344-351

[43] R. malik, D.S ramteke and S.R Wate,. Waste management V27, 9 **(2007)** 1129-1138

[44] I.D Mall, V.C Srivastava, N.K Agarwal, I.M Mischra. Colloids and Surfaces A 264 **(2005)** 17-28

[45] B. Emrah, O. Mahmut and sengil, I. Ayan,. Microporous and Mesoporous Materials V115 **(2008)** 234-246

[46] K.V Kumar and S. Sivanesan,. Dyes and pigments V21,1 **(2007)** 124129

[47] G. Renmin, F. Min, Z.Jiajing, C.Wenkai and L. Lingling. Bioresource Technology V100, 2 **(2009)** 975-978

[48] H. Oualid, S.Fethi, C. Mahdi and N. Emmanuel, Chemical Engineering Journal V143,1-3 **(2008)** 73-84